T H E U N I V E R S I T Y O F M I C H I G A N

COLLEGE OF ENGINEERING
Department of Nuclear Engineering

Final Report - Part 4

ESR OF VANADIUM IN CaO AND MgO

G. H. Azarbayejani
N. Mahootian
C. Kikuchi

ORA Project 04385

under contract with:

NATIONAL SCIENCE FOUNDATION
GRANT NO. G-15912
WASHINGTON, D.C.

administered through:

E OF RESEARCH ADMINISTRATION ANN ARBOR

September 1963

UMR0160

TABLE OF CONTENTS

LIST OF TABLES

LIST OF FIGURES

ABSTRACT

Spin resonance measurements of CaO and MgO single crystals containing vanadium and other impurities of the 3d transition elements have been carried out. The usual spin Hamiltonian coefficients have been measured at room temperature. They are: $g = 1.9678$, $A = -75.97 \times 10^{-4}$ cm^{-1}* in CaO and $g = 1.980$ and $A = -74.19$* in MgO respectively. An anisotropy due to both fine and hyperfine components has been observed and discussed.

*Others[5] have reported $A'_{MgO} = 75.2 \times 10^{-4}$ cm^{-1}. The product of 74.19 by $(g_{free}/g_{ion})_{MgO}$ gives

$A'_{MgO} = -75.2 \times 10^{-4}$ cm^{-1}, also $A'_{CaO} = -75.97 \times \frac{g_{free}}{g_{ion}} = -77.30 \times 10^{-4}$ cm^{-1}.[6]

I. INTRODUCTION

The electron spin resonance (ESR) of V^{++} ion in MgO has been reported by a number of earlier investigators.[1-5] Low[2] reports the presence of a very small rhombohedral distortion at V^{++} site in MgO being similar to that at the Mn^{++} site in this crystal. In addition it is observed[6] that the positions of the fine-structure components of V^{++} ion do not agree with the predictions of the usual spin Hamiltonian* provided only corrections of up to second order are included. Ham and others[7] have reported an improved spin Hamiltonian for $S = 3/2$ (Co^{++}) system in a cubic field containing terms of the third power in electron spin components, S_x, S_y, and S_z. This Hamiltonian produces an angular dependence of the fine structure components and it can be applied in our case. (The ground state of Co^{++} in tetrahedral compounds is the same as the ground state of V^{++} in octahedral $A_{II}B_{IV}$ compounds.)

The purpose of this report is to give a detailed investigation of the ESR of V^{++} in CaO and MgO crystals. Besides the ESR of V^{++} and V^{4+} ions in MgO powders is studied to augment the results in the crystals. Since the discrepancy in the position of the fine structure component of V^{++} ion[6] caused by contributions from higher orders of approximation and these contributions depend on the microwave frequency band, we have performed our meas-

---

* $\mathcal{H} = g\beta \underline{S} \cdot \underline{H} + A' \underline{S} \cdot \underline{I}$.

urements at X-, Ku- and K-band spectrometers.

The experimental procedures and the results are given in Section II and a discussion of the anistropy, asymmetry and line broadening of the fine structure components is given in Section III.

II. EXPERIMENTAL PROCEDURE

A. GENERAL

Samples of these crystals have been placed in the cavity so that the d-c magnetic field could be rotated in one of its (110) and (100) planes. X-band measurements are made with both rectangular TE012 and cylindrical TE011 lavite cavities[9] when at Ku- and K-band measurements only cylindrical TE011 cavities have been used. The magnetic field is produced with a rotating base 12 in. Varian magnet and the field modulation of 100 kcps has been used. The microwave frequency is determined by zero heating against the harmonics of a Beckman 7580 transfer oscillator whose frequency in turn is measured by a Beckman 7370 counter.

Magnetic field measurements are made with a Varian F-8 fluxmeter. Calibration of the field as accomplished with the resonance of polycrystalline diphenyl picryl hydrazyl with $g = 2.0036$.

B. CaO:V

Single crystals of this material which are colorless and slightly hydroscopic are obtained from Semi-Elements, Inc. Pieces of the sizes of 1 x 4 x 4 mm are used for both X- and Ku-band measurements when at K-band a piece of the sizes 1 x 2 x 2 mm is used. All of these crystals contain manganese as a natural impurity and therefore the spectra of ESR of V^{++} ion in these crystals are mixed with those of Mn^{++}. In Fig. 1 the spectra of V^{++} and Mn^{++} at Ku-band and at about 77°K is shown. The angle Θ in this figure and all others represents the angle between the d-c magnetic field H and one of the

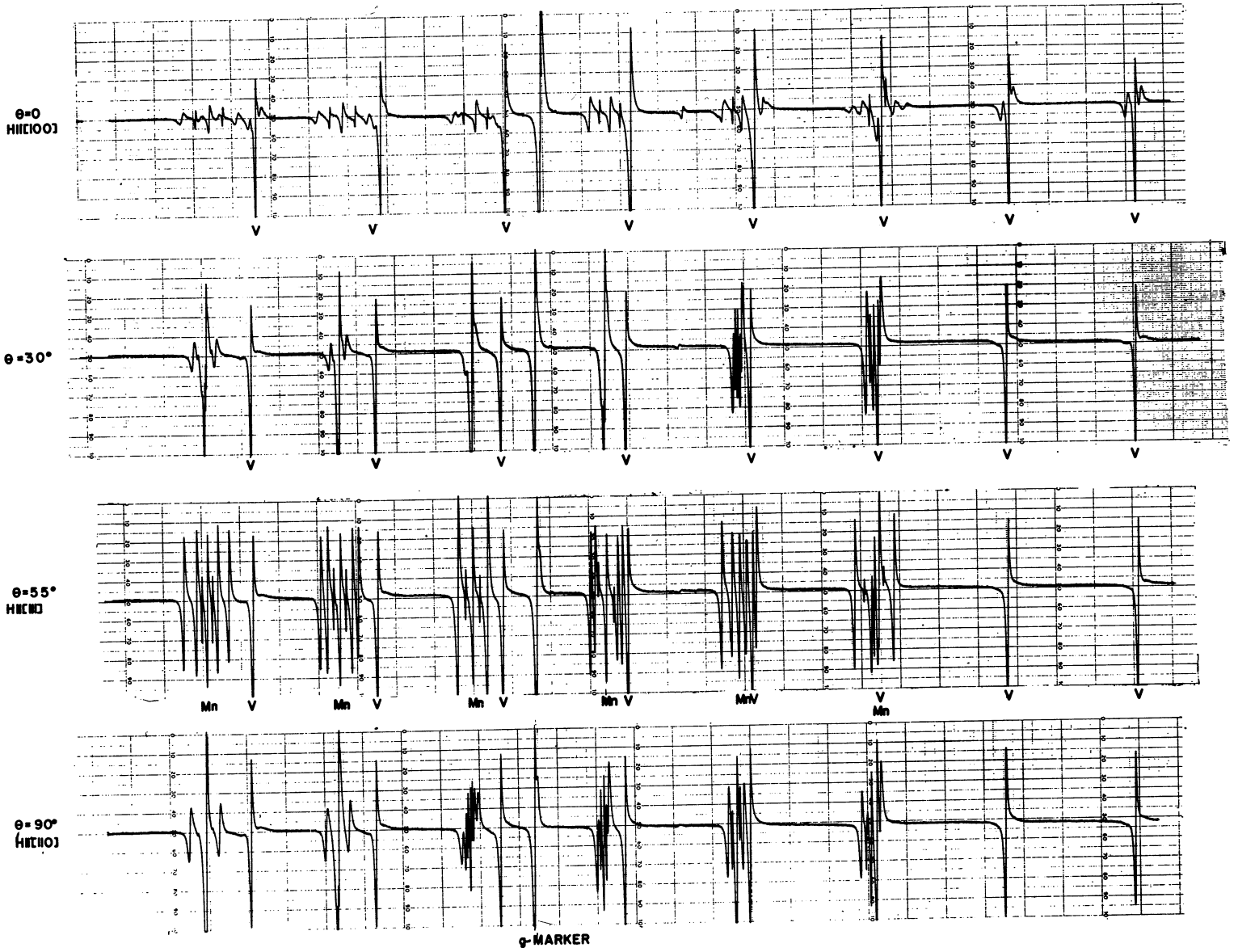

Fig. 1. ESR spectra of V^{++} and Mn^{++} in CaO at different angles.

principal axes of the cube, [100]. The angle has been determined by comparing the spectra of Mn^{++} in these crystals with those in a standard sample of MgO. The standard sample has been examined by X-ray diffraction and the result indicates that the faces of these crystals are mostly in (100) planes. The assumption that the cleavage planes of the CaO samples are of the (100) type was confirmed by the symmetry of the ESR spectra of Mn^{++} in these samples. Since in all of the samples we have used, the manganese impurity is present, we have been able to determine θ within 1°. In Fig. 2 the spectra at $\theta = 0$ and at about 9, 18, and 24 G/sec are shown. The samples S102; S101 and S102R are of the same source and R in S102R indicates irradiation with X-rays. A comparison of these spectra shows that the second order effects are the major mechanisms responsible for the splitting of the lines of V^{++} ions. To determine these effects as a function of different parameters the measurements at X-band was investigated in more detail. In Fig. 3 the angular variation of the line in extreme left of Fig. 2a is shown. This line, V_8, corresponds to the V^{++} ion for nuclear magnetic quantum number $m = 7/2$. The variation in the (110) plane of the crystal S101 (Fig. 3a) indicates that the fine structure components α and γ (see Fig. 14) are sharpest along the [100] directions where they are broadest along the [111] directions. In the (100) planes the general trend is the same but the components α and γ (Fig. 3b) are not smeared off completely as in the (110) plane. To investigate the same phenomenon as a function of lattice constant a_o it was necessary to run crystals of MgO containing vanadium impurity. The results are as follows.

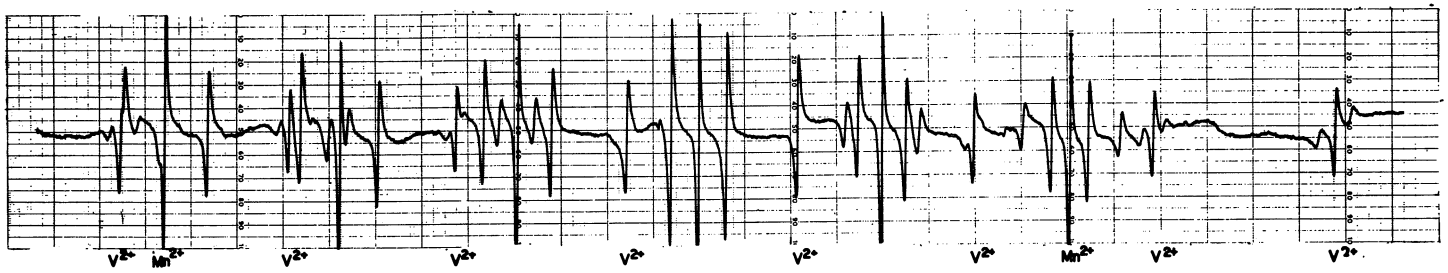

a. X-BAND

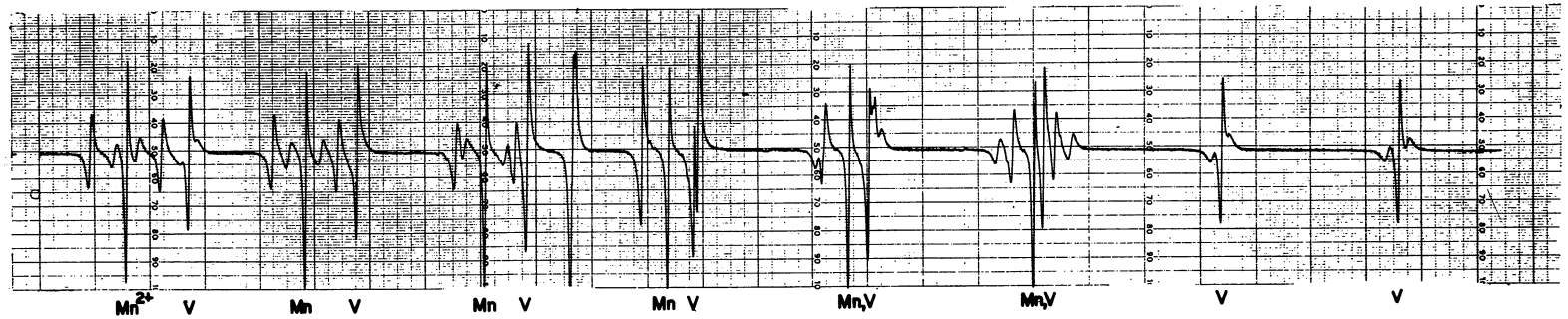

b. Ku-BAND

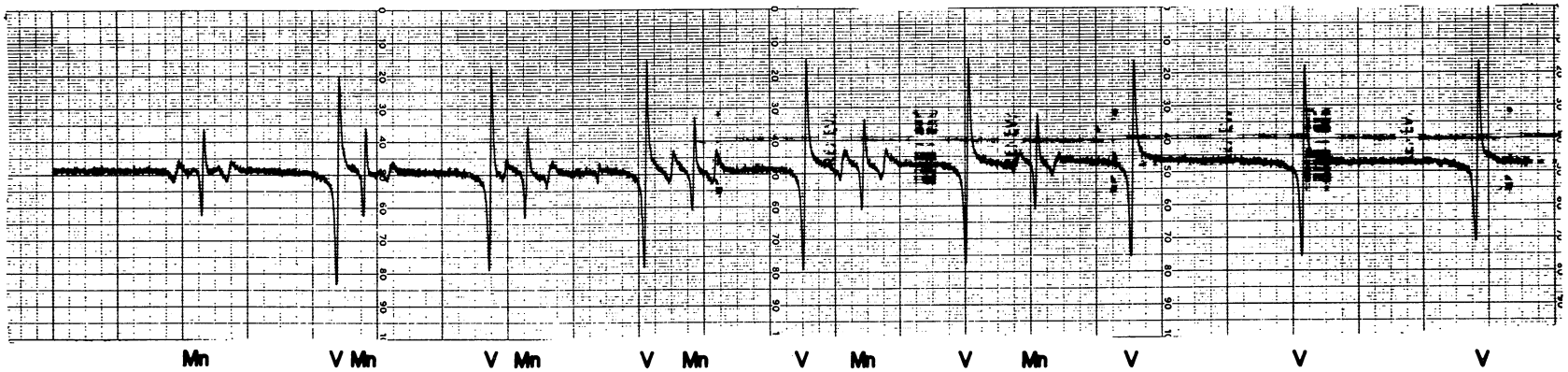

c. K-BAND

Fig. 2. ESR spectra of V^{++} and Mn^{++} in CaO at different frequency bands and at $\Theta=0$ ($H \| [100]$).

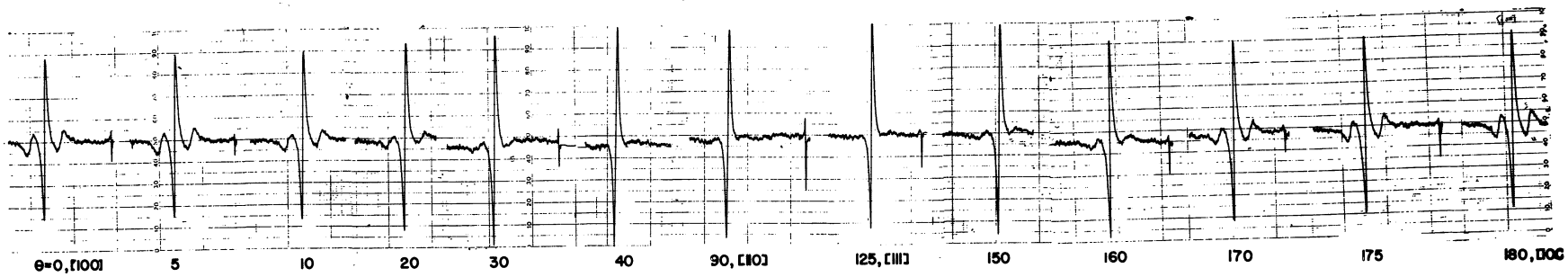

a. (110) PLANE

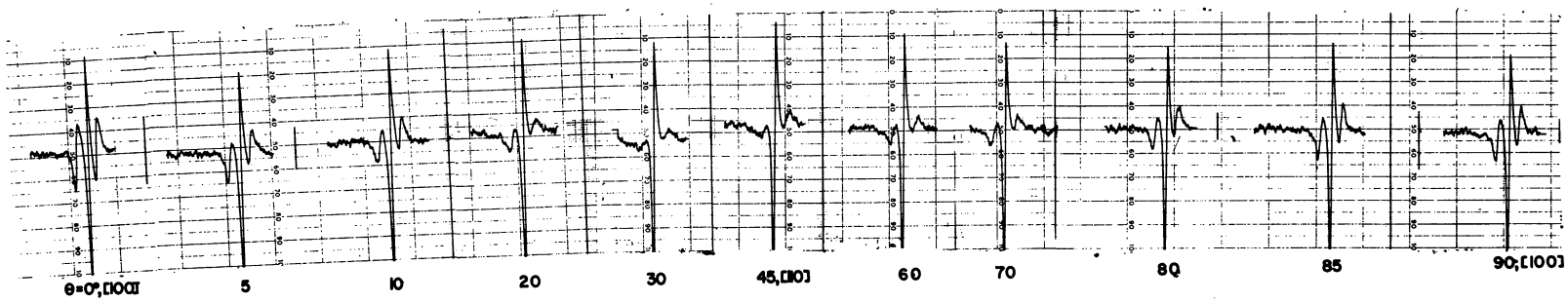

b. (100) PLANE

Fig. 3. Angular variation of the spectrum of V_8^{++} (m=7/2) in CaO.

C. MgO:V (CRYSTAL)

As in the case of CaO most of the samples available to us contain an appreciable amount of other impurities such as manganese, chromium and iron. The spectra of V^{++} can be, however, enhanced by irradiating the crystals with X-rays for a few hours. The spectra of V^{++}, Mn^{++}, and Fe^{+++} in MgO are given in Fig. 4. The fine structure components of V^{++} is very well resolved along [100] directions (Fig. 4a) whereas along [111] and [110] directions they are smeared off (Figs. 4c and 4d). The spectrum at $\Theta = 0$ in which the two components α and γ (Fig. 4a) are sharpest is taken at X- and K-band (Figs. 5a and 5c) in the samples S306 and 306. At X-band the components are clearly resolved when it is difficult to find them at K-band. It is also very interesting to note that the separation of the components with $m < 0$ is larger than the corresponding lines with $m > 0$. The angular variation of the vanadium line V_8^{++} ($m = 7/2$), (Fig. 5a) in the planes (110) and (100) (Figs. 6a and 6b) is similar to CaO, (Figs. 3a and 3b). Since one of the sources of the broadening in solid state paramagnetic resonance is the spin lattice relaxation the angular variation of V_8 in the (100) plane was investigated at liquid nitrogen temperature (Fig. 6c). It was found that the effect of temperature was unobservable. Therefore, we conclude that, in MgO:V, the spectra of V^{++} show the same dependence on the crystalline field as in CaO:V. In both of these materials a variation of the separation of the two components α and γ is observed which could not be expressed by the usual spin Hamiltonian. This point will be discussed in Section III in more detail.

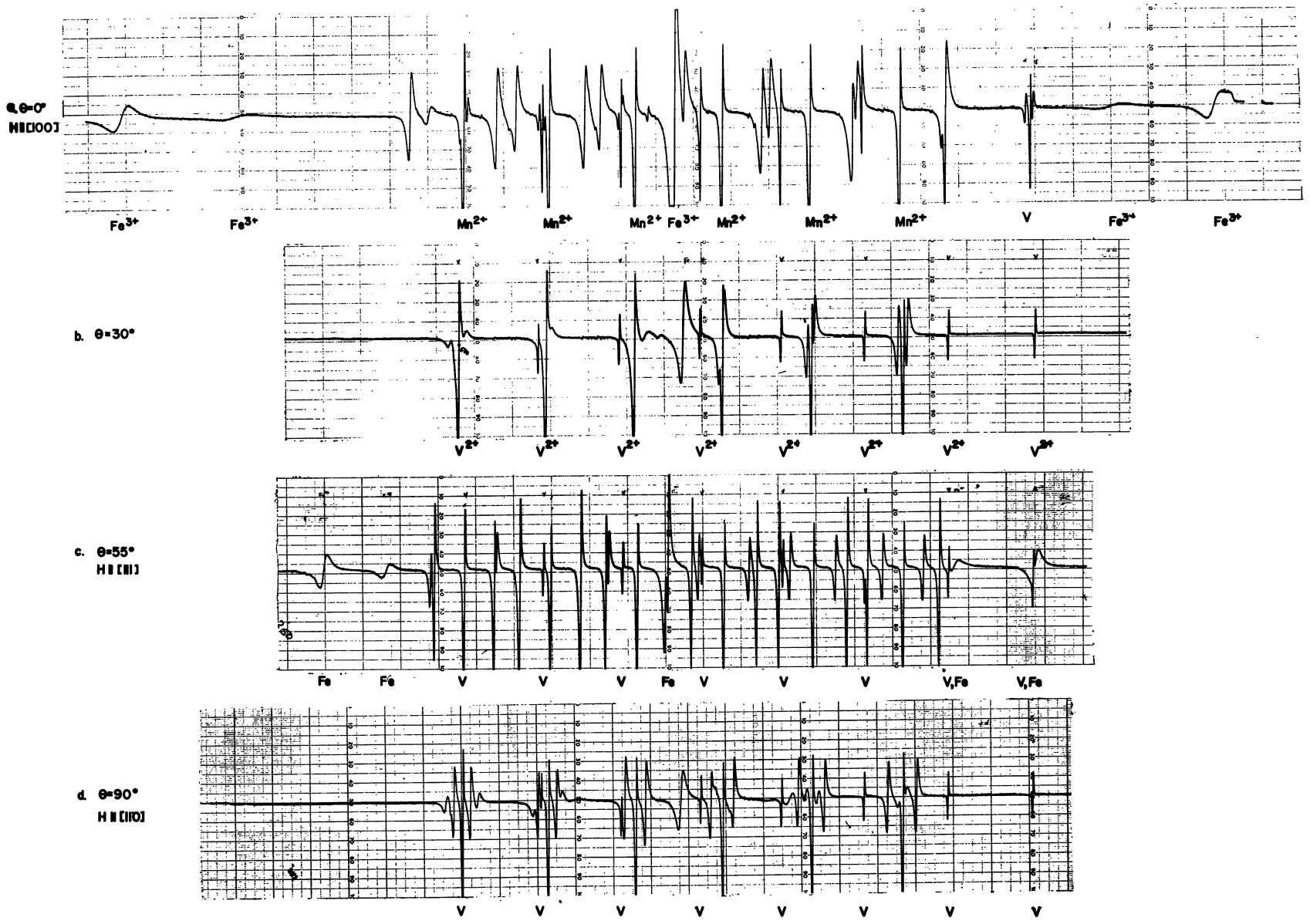

Fig. 4. ESR spectra of V^{++}, Mn^{++} and Fe^{3+} in MgO at different angles.

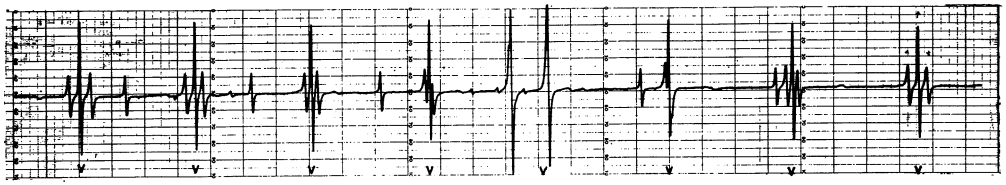

a. X-BAND

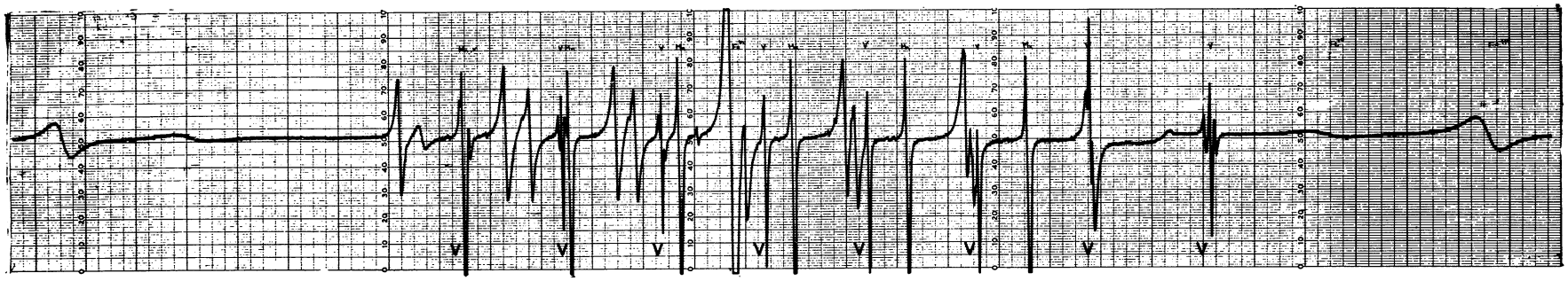

b. Ku-BAND

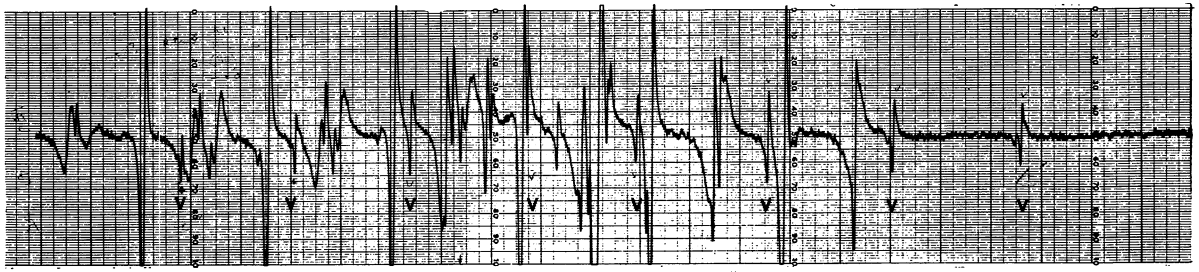

c. K-BAND

Fig. 5. ESR spectra of V^{++}, Mn^{++} and Fe^{3+} in MgO at different frequency bands and at $\theta=0$ ($H \| [100]$).

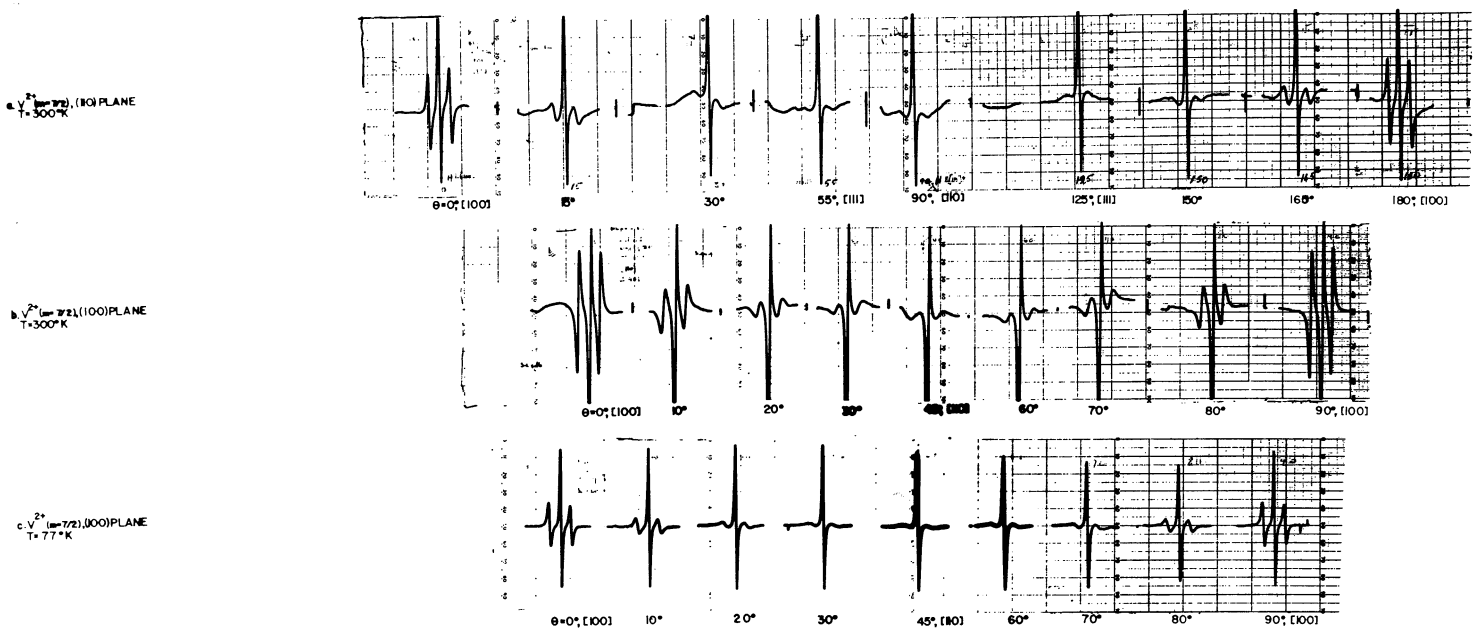

Fig. 6. Angular variation of the spectrum of V_8^{++} (m=7/2) in MgO.

D. ZnS:Mn

To obtain the origin of the broadening of the components of V_8 as a function of crystalline structure we took a spectrum of manganese in cubic ZnS in the (110) plane (Fig. 7b). A similar spectrum of Mn^{++} in CaO in the (110) plane (Fig. 7a) is taken for comparison. It is evident that the line broadening of Mn^{++} fine structure components α, β, δ, and λ in ZnS are opposite to their broadening in CaO. The angular variation of the broadening of the components α and γ of V_1 and α, β, δ, and λ of Fe^{+++} and Mn^{++} in MgO are given in Fig. 8. A comparison among the spectra in Figs. 8a-8e indicates that the broadening of V^{++} components is opposite to the broadening of the components of Mn^{++} and Fe^{+++} in MgO but is similar to the broadening of the components of Mn^{++} in ZnS. The spectra of V^{++} in tetrahedral field[10] shows a broadening which is apparently similar to the components of Mn^{++} in MgO. The numerical values of the splitting and separation of the components α and γ from each other and from the central line (β) are given in Tables I-V.

E. MgO:V POWDER SAMPLES

Powder samples were prepared by wetting MgO powder with a few drops of aquous solution of vanadyl chloride to obtain a thick dough-like mixture with an atomic relative concentration V/Mg of about 0.05%. The samples were then dried at 100-150°C and "fired" subsequently at high temperatures for several hours. Firing was done in an electric conduction furnace that could be operated at a maximum temperature of 1300°C. The fired samples were then x-irradiated at 50 KVP x 35 ma for about an hour.

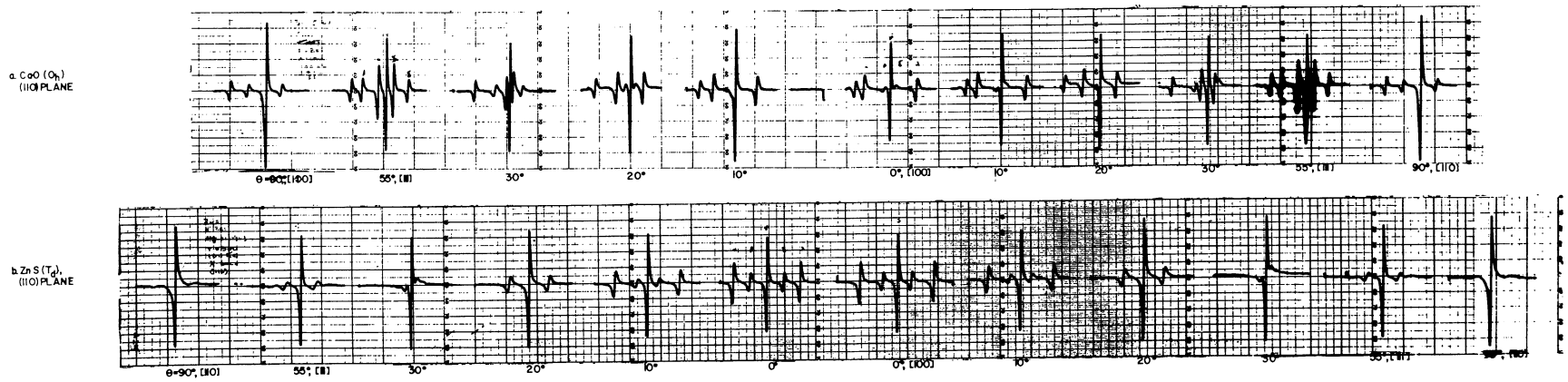

Fig. 7. Angular variation of the spectrum Mn_6^{++} (m=5/2) in CaO and ZnS.

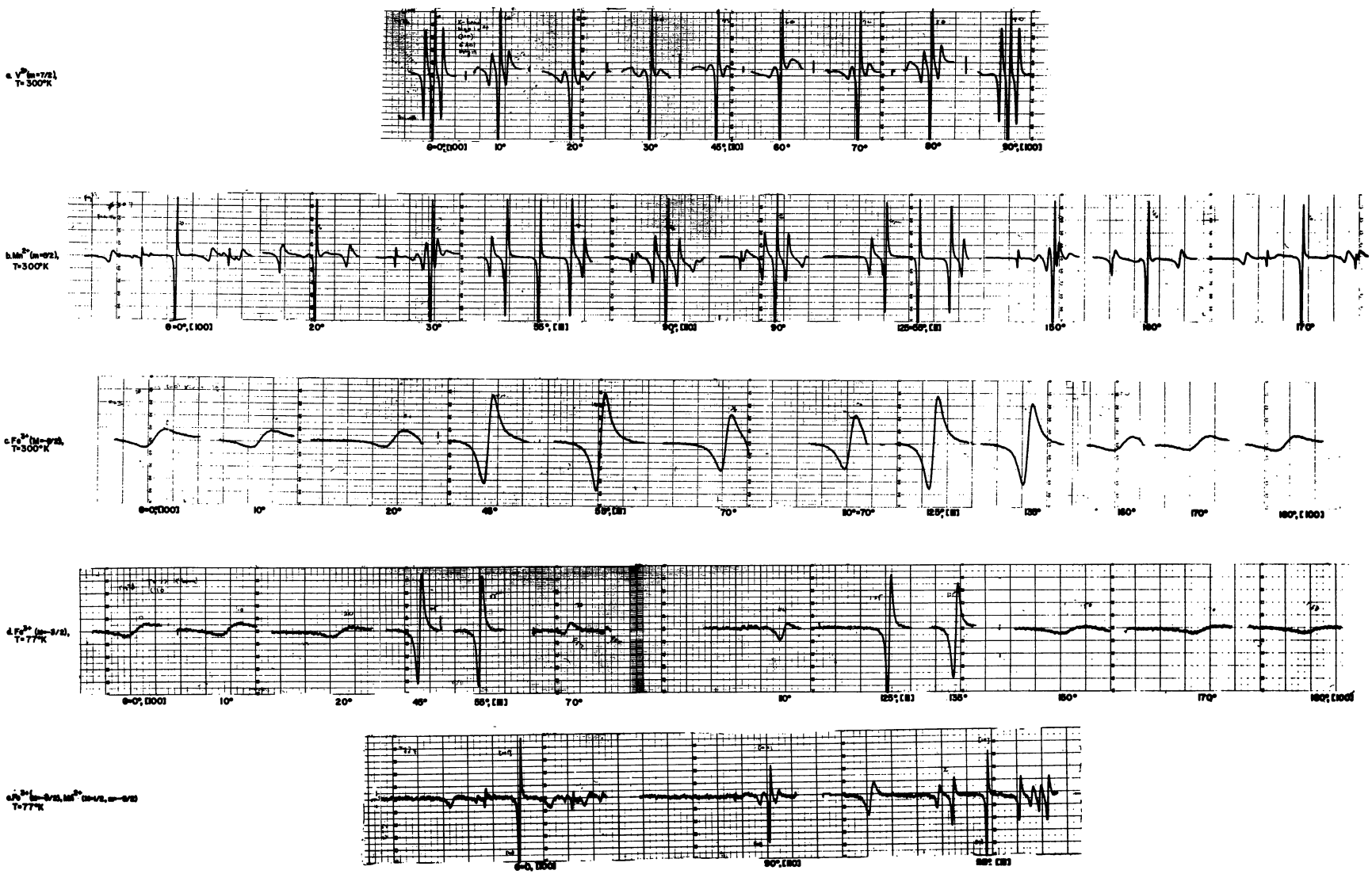

Fig. 8. Angular variation of the spectra of the V_8^{++} (m=7/2), Mn_6^{++} (m=5/2) and Fe^{3+} in MgO.

The spectra of the powder samples depend on the heat treatment as follows:

(a) Samples fired at 700-1000°C in air do not show any vanadium spectra either at 300° or at 77°K prior to x-irradiation. After the irradiation a set of eight sharp lines* (line width about 1.2 gauss) about g = 2. The lines are separated by 77-83 gauss and do not have any satellites (Fig. 9a).

(b) Samples fired at about 1000°C in a reducing atmosphere such as hydrogen show, after x-irradiation, an ESR spectrum which contains a set of eight lines, each flanked by two satellites (Fig. 9b). The line width and position of the central lines in the magnetic field are quite the same as in (a). The separation of the satellites from each other depends on location of the corresponding central line (Table V), similar to the case of the single crystal samples.

(c) Samples fired at 1200-1300°C in air show no spectra, before irradiation, either at 300° or at 77°K. Upon x-irradiation, an ESR spectrum, similar to (b), is obtained.

(d) Finally, samples fired at 1200-1300°C in an oxidizing atmosphere and x-irradiated subsequently show an ESR spectrum similar to (a), i.e., a set of eight sharp lines without any accompanying satellites.

The above observations lead us to believe that the set of lines in (a) and (d) can be associated with V^{4+} (I = 7/2, S = 1/2) ions. In (b) and (c)

*These are in addition to the characteristic lines of Mn^{++}, Fe^{+++}, and Cr^{+++} which are present as impurities in the magnesium oxide powder used in preparation of our samples.

Fig. 9. ESR spectra of vanadium in MgO powder.

however, the two satellites flanking each hfs principal line suggests that the electron spin of the paramagnetic center is 3/2, and thus vanadium must be in V^{2+} state. In fact, very good agreement between theory and experiment is obtained by assuming that the satellite splitting is due to second-order effects in the electron-nuclear interaction term. Our tentative conclusion receives further support from the fact that ESR spectrum of the single crystal $MgO:V^{2+}$ samples in the [100] direction is quite similar to those of the powder samples in (b) and (c).

Further investigations are being made to determine the mechanism of temperature and radiation effects in powder samples.

TABLE I

ANGULAR VARIATION OF THE COMPONENTS α, β, AND γ OF V^{++} IN THE (110) PLANE OF CaO:V [a]

Line	θ	α	β	γ	$\Delta_{\beta\alpha}$	$\Delta_{\gamma\beta}$	$\Delta_{\gamma\alpha}$
V_8^{++} (m = 7/2)	0°	1394961[b]	1398100[b]	1400931[b]	7.37[c]	6.65[c]	14.02[c]
	15°	1395029	o398103	1400931	7.22	6.64	13.86
V_7^{++} (m = 5/2)	0°	1361935	1364162	1365970	5.23	4.25	9.48

[a] Unless specified the data are taken at X-band.
[b] In arbitrary unit.
[c] Δ_{ij} is the separation of the two components i and j in units of gauss.

TABLE II

ANGULAR VARIATION OF THE COMPONENTS α, β, AND γ OF V_8 IN THE (100) PLANE OF MgO:V

θ	$\Delta_{\beta\alpha}$	$\Delta_{\gamma\beta}$	$\Delta_{\gamma\alpha}$	$\Delta_{\gamma\alpha}/2$
0°	6.72	6.08	12.80	6.40
15°	6.62	6.43	13.05	6.52
30°	6.41	6.87	13.28	6.64
45°	6.64	7.02	13.67	6.83
60°	6.41	6.78	13.20	6.60
75°	6.64	6.27	12.91	6.45
90°	6.77	6.08	12.85	6.42

TABLE III

$\Delta_{\gamma\alpha}$ IN THE (100) PLANE OF MgO:V AS A FUNCTION OF m AND θ

m → θ ↓	-7/2	-5/2	-3/2	-1/2	5/2	7/2
0°, [100]	14.09	11.25	8.24	3.43	7.8	12.87
45°, [110]	13.35	12.06	9.55	-	-	-

TABLE IV

ANGULAR VARIATION OF V_8 COMPONENT

IN THE (110) PLANE OF MgO:V

θ	$\Delta_{\beta\alpha}$	$\Delta_{\gamma\beta}$	$\Delta_{\gamma\alpha}$
0°	6.60[a]	5.84	12.44
15°	6.02	5.70	11.72
30°	5.62	5.82	11.44
55°	5.73	6.54	12.27
90°	5.40	6.33	11.73

[a]All values are in gauss.

TABLE V

$\Delta_{\gamma\alpha}$ AS A FUNCTION OF m IN POWDER SAMPLES

(Ku-BAND SPECTRUM) AT ν_o = 17.136 KMC/SEC

m	-7/2	-5/2	-3/2	-1/2	1/2	3/2	5/2	7/2
Central Line	V_1	V_2	V_3	V_4	V_5	V_6	V_7	V_8
Gausses	7.2	5.6	4.6	-	-	-	-	-

III. DISCUSSION

A. LINE POSITION

The position of the V^{2+} lines can be expressed in terms of the magnetic field H as (see Appendix A, Section 1)

$$H_{(M=3/2\rightarrow M=1/2)} = (1+1.2up/g)^{-1}\left[H_o - A(1+1.2Up/A)m + \frac{A^2}{H_o}m\right] - \Delta_1(m,\theta) \quad (1)$$

$$H_{(M=1/2\rightarrow M=-1/2)} = (1+1.8up/g)^{-1}\left[H_o - A(1-1.8Up/A)m\right] \quad (2)$$

$$H_{(M=-1/2\rightarrow M=-3/2)} = (1+1.2up/g)^{-1}\left[H_o - A(1+1.2Up/A) + \frac{A^2}{H_o}m\right] - \Delta_2(m,\theta) \quad (3)$$

where $H_o = h\nu_o/g\beta$, u and U are constant coefficients, and p is defined by

$$p = 1 - 5(n_1^2 n_2^2 + n_2^2 n_3^2 + n_3^2 n_1^2) \quad (4)$$

With n_1, n_2, and n_3 being the direction cosines of the magnetic field with respect to the three cubic axes.

$\Delta_1(m,\theta)$ and $\Delta_2(m,\theta)$ in (1) and (3) denote the discrepancies between the experimental values of line position and the calculated ones. Higher order perturbations caused by hyperfine interaction make substantial contribution to Δ_1 and Δ_2.

The value of u and U, obtained from Eq. (2), are

$$u \simeq 3 \times 10^{-5}, \quad U \simeq 10^{-6}\ \text{cm}^{-1}$$

A major contribution to u and U comes from the fourth order perturbation[8] caused by the spin-orbit interaction term $\lambda \underline{L}\cdot\underline{S}$ together with the Zeeman term $\beta(\underline{L}+2\underline{S})\underline{H}$, or with the hyperfine interaction term $P(\underline{L}\cdot\underline{I})$. Denoting these contributions by u_1 and U_1, they are found to be (see Appendix A, Section 2, Eqs. (A.22) and (A.23))

$$u_1 = 120\ \lambda^3/(E_{52}^2 E_{42}) \tag{6}$$

and

$$U_1 = Pu_1 \tag{7}$$

where λ is the spin-orbit coupling constant, $E_{52} \equiv E_{\Gamma_5} - E_{\Gamma_2}$, and $E_{42} \equiv E_{\Gamma_4} - E_{\Gamma_2}$. Substituting for λ, E_{52}, and E_{42} one obtains:[11,12]

$$u_1 = 120(90)^3/(13200^2 \times 19900) \simeq 2.8 \times 10^{-5}$$

and

$$U_1 \simeq 10^{-6}\ \text{cm}^{-1} \tag{8}$$

Ham *et al.*,[8] have used the first two terms of Eqs. (1) and (3). They have neglected the third term apparently because its effect on the line position of Co^{2+} in CdTe is at most 0.14 gauss to be compared with U ≃ 1 gauss. In our case, however, both the third and the fourth terms of these equations are necessary to describe the position of V^{2+} lines in the octahedral field.

To obtain the magnitude of Δ_1 and Δ_2 (Eqs. (1) and (3)) we consider Fig. 10 and Eqs. (1)-(5). Equation (5) indicates that at $\theta = 30°$ and in (100) planes

$$p = 1 - 15/16 \simeq 0 \tag{9}$$

and

$$(up/g)H < 3 \times 10^{-5} \times 3 \times 10^{3} \times 6 \times 10^{-2} \simeq 0.005 \text{ gauss} \tag{10}$$

and

$$Up \simeq 10^{-6} \times 6 \times 10^{-2} \simeq 0.0007 \text{ gauss} \tag{11}$$

These quantities are certainly negligible compared to the deviations of the position of the components α and γ as illustrated by Figs. 10-12. The Eqs. (1)-(3) can, therefore, be re-written neglecting the terms having up and Up:

$$H(M = 3/2,m,30°) = H_0 - Am + mA^2/H_0 - \Delta_1(m,\theta) \tag{12}$$

$$H(M = 1/2,m,30°) = H_0 - Am \tag{13}$$

$$H(M = -1/2,m,30°) = H_0 - Am - mA^2/H_0 - \Delta_2(m,\theta) \tag{14}$$

whence

$$|H(M = 3/2,m,\theta=30°) - H(M = -1/2,m,30°)| = |2mA^2/H_0 - (\Delta_1-\Delta_2)| \tag{15}$$

Assuming $A < 0$, as is obtained from nuclear magnetic moment measurements, the Zeeman splittings of V^{++} nuclear and electronic spin levels is shown in Fig. 13. Therefore the components α and γ of V_1 and V_8 in Fig. 7 can be designated as in Fig. 14. Here m is the nuclear magnetic quantum number and assignment of M to -1/2, 1/2, and 3/2 is according to Kikuchi's designa-

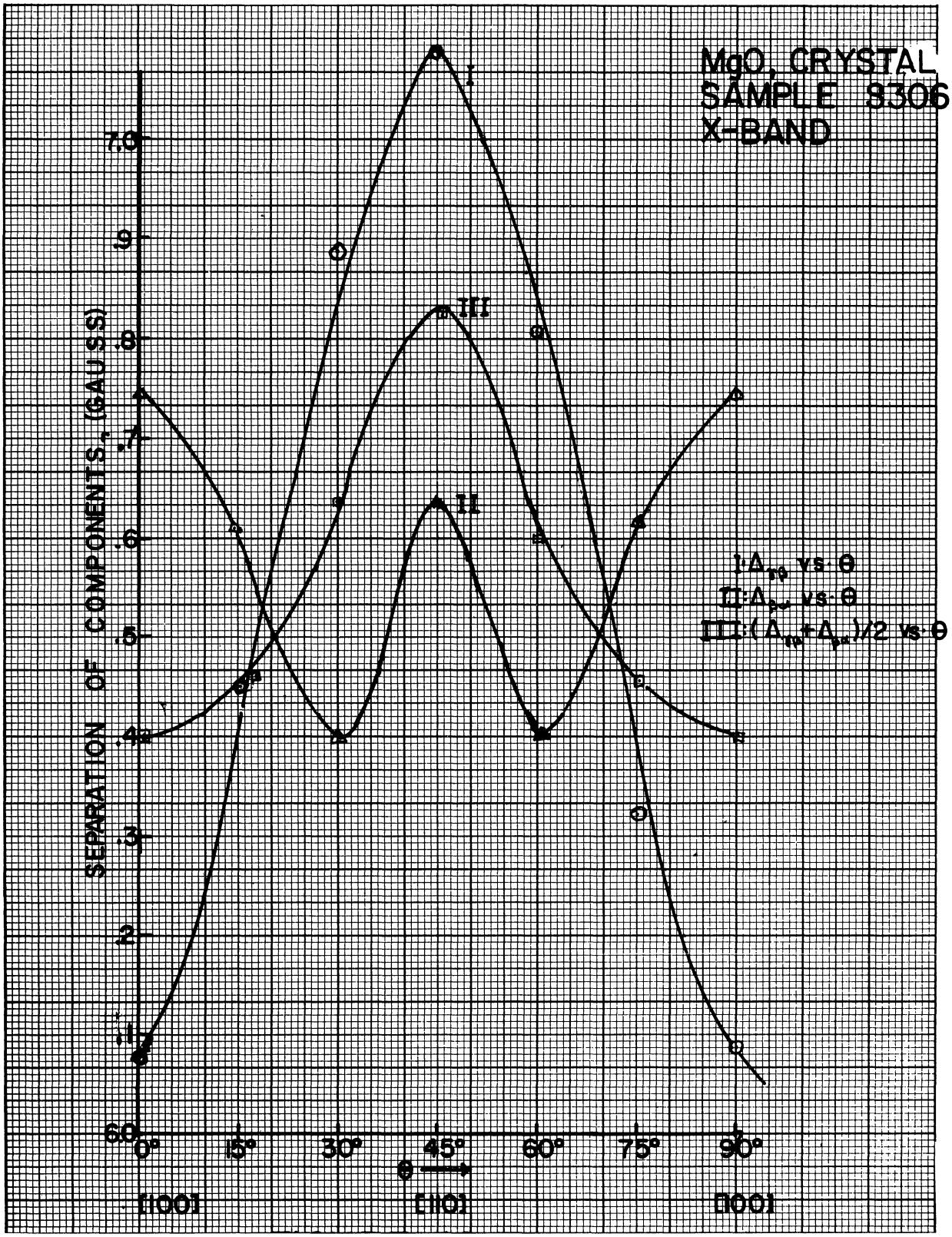

Fig. 10. The angular variation of the components α, β, and γ in the plane (100) of MgO (S306).

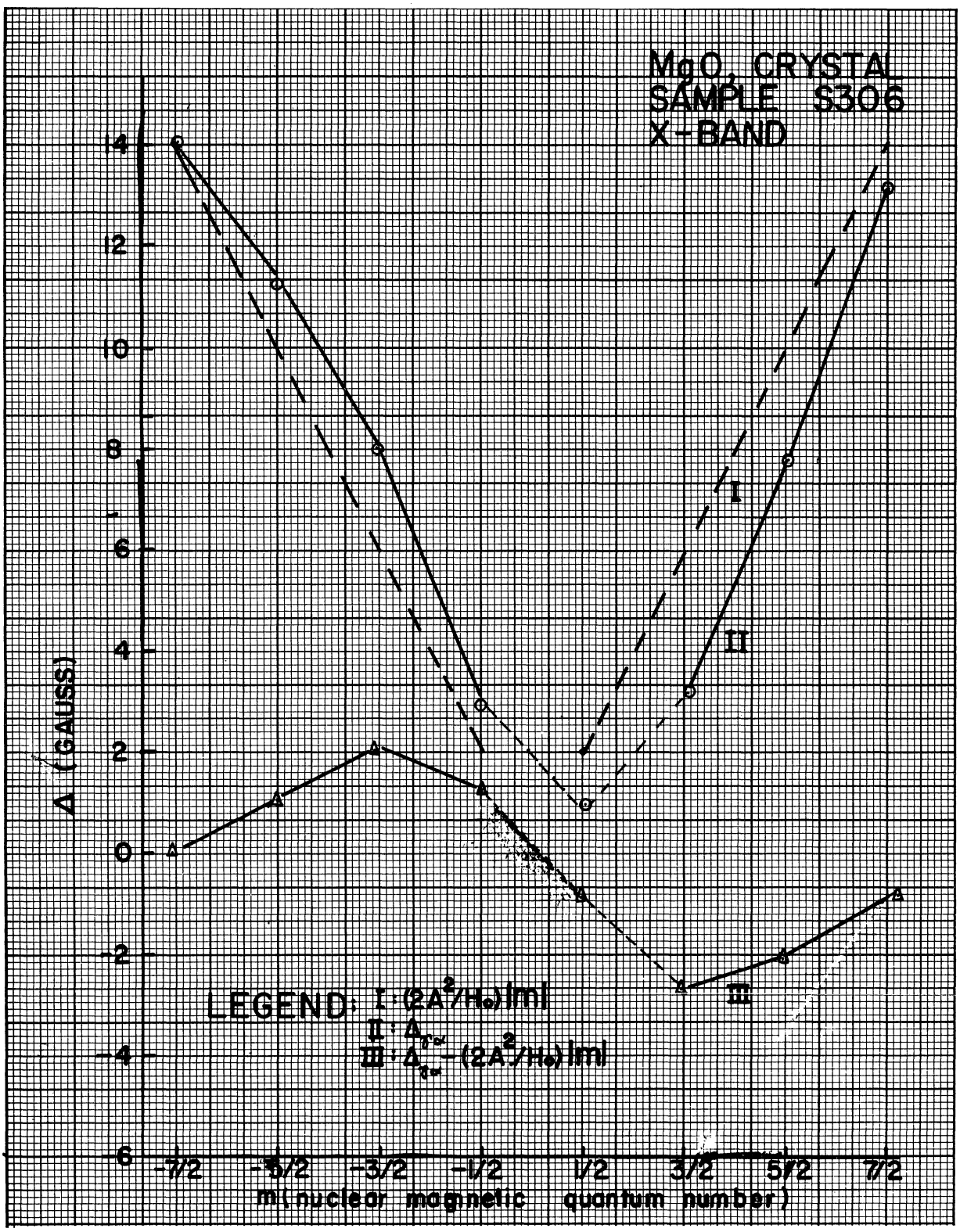

Fig. 11. Variation of the separation of the components α and γ vs. m at X-band and at Θ=0 of the (100) plane of MgO (S306).

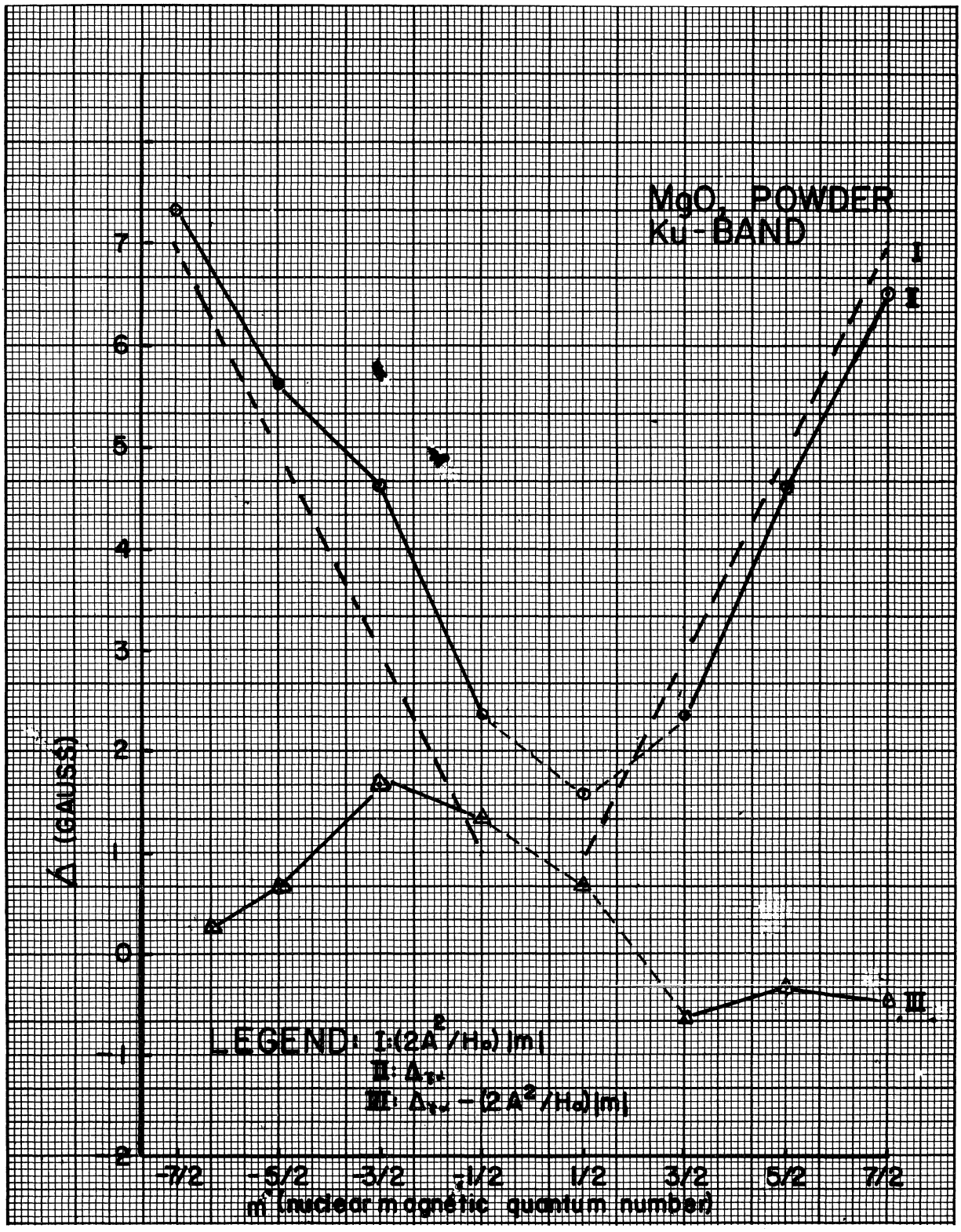

Fig. 12. $\Delta_{\alpha\gamma}$ vs. m at Ku-band in the powder of MgO.

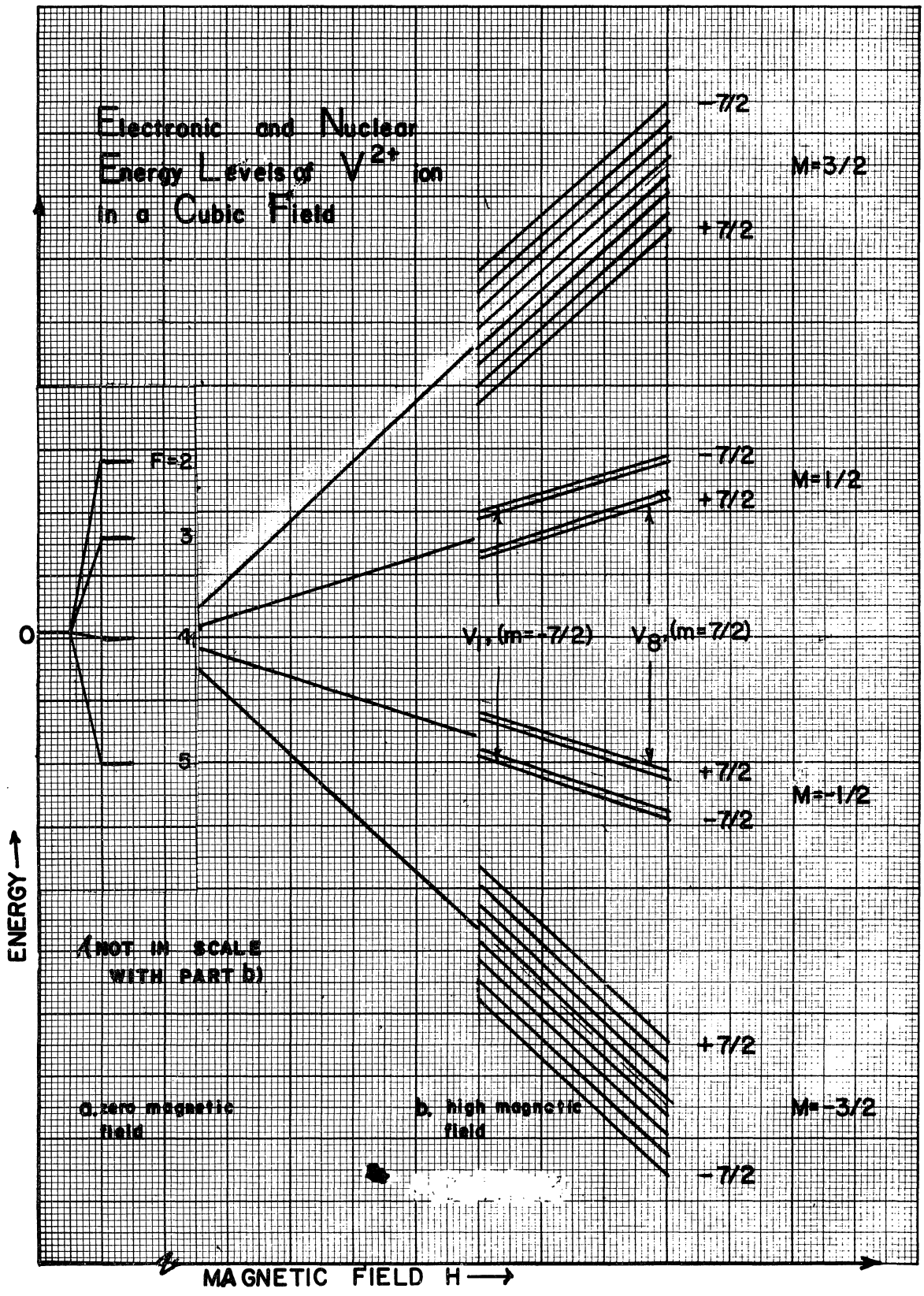

Fig. 13. Zeeman splittings of V^{++} electronic and nuclear spin levels.

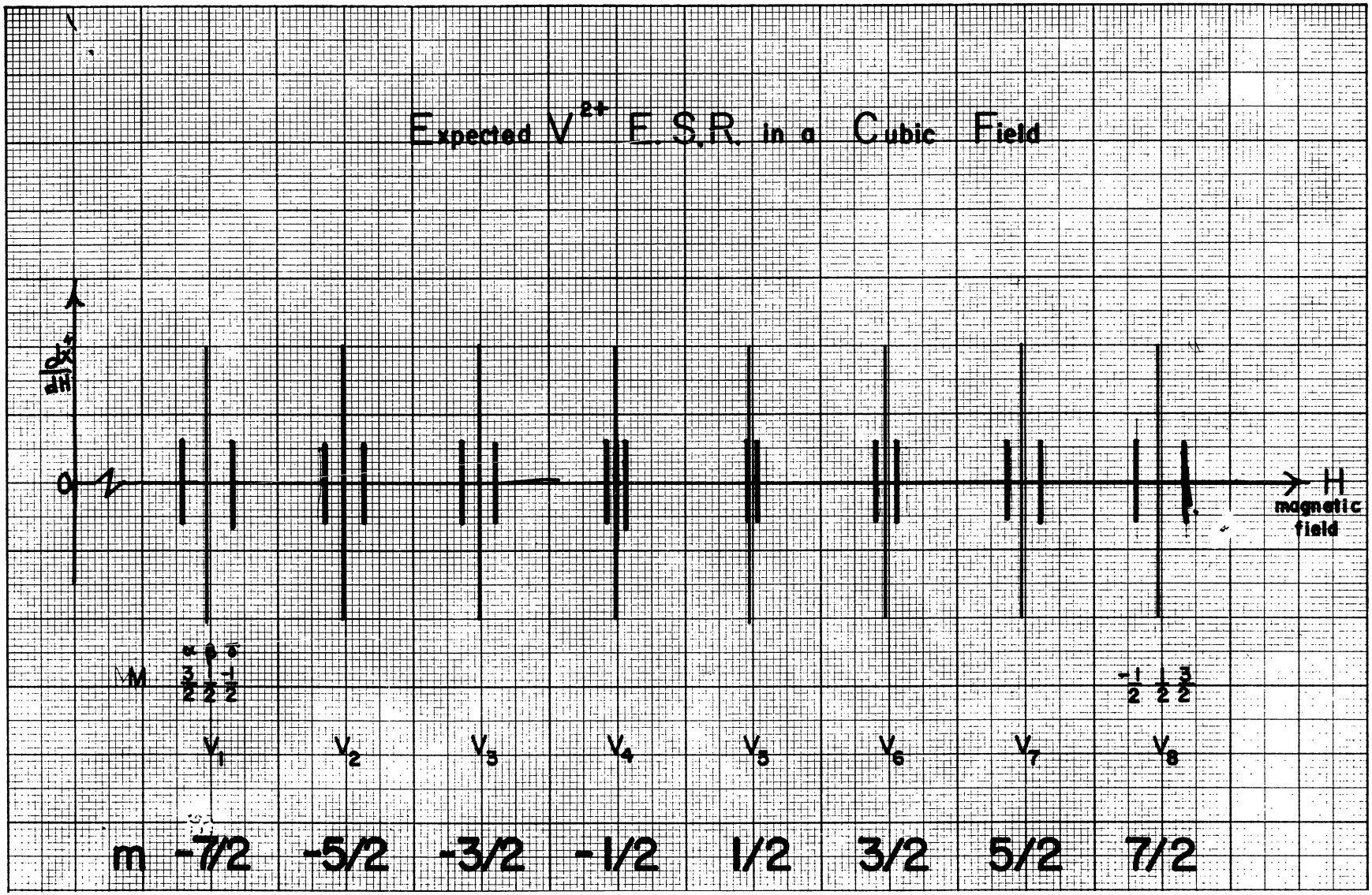

Fig. 14. Designation of the components of the expected V^{++} ESR in a cubic field.

tion. Thus, for $V_8(m = 7/2)$, Eq. (15) gives:

$$2\sigma = [H(M = 3/2, m = 7/2, \Theta=30°) - H(M = -1/2, m = 7/2, \Theta=30°)] = |7A^2/H_o - (\Delta_1 - \Delta_2)| \quad (16)$$

where:

$$2\sigma = 13.30 \text{ (gauss)} \quad (17)$$

and

$$7A^2/H_o = 13.51 \text{ (gauss)} \quad (18)$$

Equations (16)-(18) give

$$(\Delta_1 - \Delta_2) \simeq 0.21 \text{ (gauss)} \quad (19)$$

Equations (12) and (13) give:

$$\Delta_{\gamma\beta}(\Theta=30°, m=7/2) = \frac{7}{2} A^2/H_o - \Delta_1(7/2, 30°) \rightarrow \Delta_1 = -0.13 \text{ gauss} \quad (20)$$

and

$$\Delta_{\beta\alpha}(\Theta=30°, m=7/2) = \frac{7}{2} A^2/H_o + \Delta_2(7/2, 30°) \rightarrow \Delta_2 = -0.35 \text{ gauss} \quad (21)$$

Considering Eqs. (9)-(11) and (19)-(21) one finds that the parameters u and U at most would do a contribution smaller than 0.1 gauss when both Δ_1 and Δ_2 are larger than 0.10 gauss. The dependence of the parameters Δ on m is more pronounced for smaller m as shown in Figs. 11 and 12.

B. LINE BROADENING

Our investigations concerning the line broadening suggest that charge transfer may account for this phenomenon provided we assume that in case of Mn^{++} and Fe^{+++} the transfer takes place, through σ-bonding and e orbitals of $t_2^3e^2$ configurations of these ions. But in case of V^{2+} only through t_2^3 orbitals. This mechanism explains why the Mn^{++} and Fe^{+++} ESR spectra in ZnS show similarity with that of V^{++} in MgO and CaO and the spectrum of V^{++} in silicon shows similarity with Fe^{+++} and Mn^{++} in MgO and CaO.

C. IRRADIATION RESULTS

Irradiating MgO and CaO with X-rays we have been able to increase Fe^{+++} and V^{++} populations. These ions, however, anneal as is shown by Fig. 15.

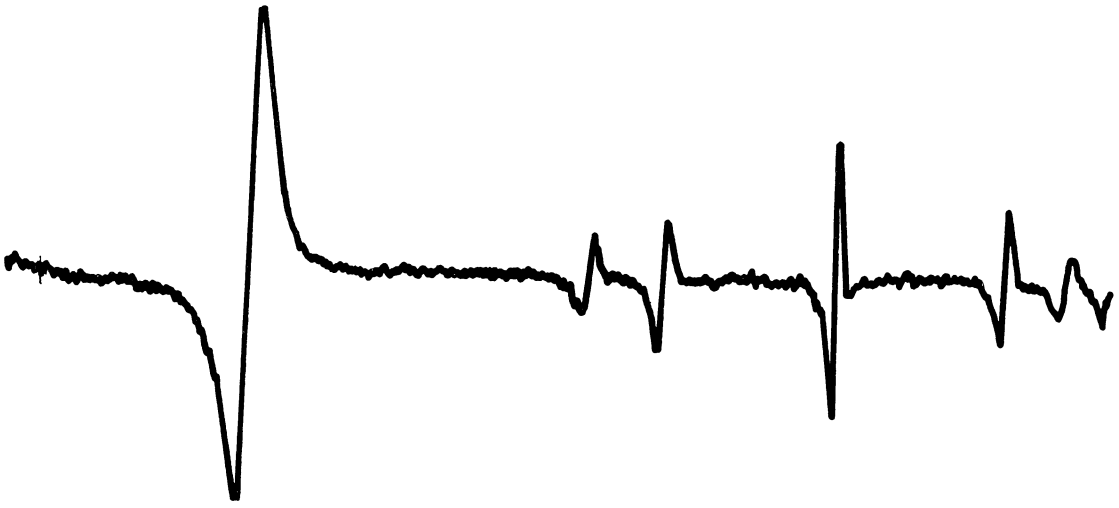

a. 7 hrs. AFTER IRRAD.

b. 30 hrs. AFTER IRRAD.

Fig. 15. X-ray irradiation of MgO:Fe, V, Mn.

IV. NEW RESULTS

In addition to the usual fine lines in each of the six groups of the Mn^{++} ESR spectrum in CaO (Fig. 3, $\theta = 55°$) we observe two extra components in each group. These components are tentatively assigned to Mn^{4+}. Further investigations are necessary to identify these lines.

ACKNOWLEDGMENTS

The authors wish to thank Dr. H. Watanabe for his valuable discussions and helpful comments.

APPENDIX A

1. DERIVATION OF V^{2+} LINE POSITION

The spin Hamiltonian for $S \leq 2$ ions in a crystalline field of cubic or tetragonal symmetry is usually written as

$$\mathcal{H}_s^{(o)} = g\beta \underline{S}\cdot\underline{H} + A'\underline{S}\cdot\underline{I} - g_N\beta_N\underline{I}\cdot\underline{H} \qquad (A\text{-}1)$$

However, this simple spin Hamiltonian cannot explain the angular variation of ESR spectra that we have observed. Similar observations have been reported by others.[14,8] As Bleaney[15] and Koster and Statz[16] have suggested, there are cases where some of the observed anomalies can be accounted for by addition of a correction term to $\mathcal{H}_s^{(o)}$. This correction term is given by

$$\Delta\mathcal{H}_s = u\beta\{S_x^3H_x + S_y^3H_y + S_z^3H_z - \frac{1}{5}(\underline{S}\cdot\underline{H})[3S(S+1)-1]\} \qquad (A\text{-}2)$$

$$+ U\{S_x^3I_x + S_y^3I_y + S_z^3I_z - \frac{1}{5}(\underline{S}\cdot\underline{I})[3S(S+1)-1]\}$$

where x, y, and z are the cubic axes of the crystal and u and U are constants depending on g. Using above additive terms and neglecting the last term of (A-1) which is very small and causes a constant shift in all energy levels, the new spin Hamiltonian can be written as

$$\mathcal{H}'_s = g\beta \underline{S}\cdot\underline{H} + A'\underline{S}\cdot\underline{I}$$

$$+ u\beta\{S_x^3H_x + S_y^3H_y + S_z^3H_z - \frac{1}{5}(\underline{S}\cdot\underline{H})[3S(S+1)-1]\} \qquad (A\text{-}3)$$

$$+ U\{S_x^3I_x + S_y^3I_y + S_z^3I_z - \frac{1}{5}(\underline{S}\cdot\underline{I})[3S(S+1)-1]\}$$

Using the corrected spin Hamiltonian $\mathcal{H}'_s$, the energy levels to second order in A and to first order in u and U are found to be

$$E_{M,m} = g\beta HM + A'mM$$

$$+ \frac{A'^2}{2g\beta H_o}[I(I+1)-m^2+m(2M-1)] \qquad (A\text{-}4)$$

$$+ (u\beta H+Um)\{M^3 - \frac{1}{5}[3S(S+1)-1]M\}p$$

where, M and m are eigenvalues of $\underline{S}$ and $\underline{I}$ along the magnetic field $\underline{H}$, H_o stands for $h\nu/g\beta$, and

$$p \equiv 1 - 5(n_1^2n_2^2 + n_2^2n_3^2 + n_3^2n_1^2)$$

with n_1, n_2, and n_3 denoting direction cosines of the magnetic field $\underline{H}$ with respect to the three cubic axes.

The position of the V^{2+} lines in gauss is found from Eq. (A-4) to be

$$H_{(M=3/2\rightarrow M=1/2)} = (1+1.2up/g)^{-1}[H_o-A(1+1.2Up/A)m + \frac{A^2}{H_o}m] \qquad (A\text{-}5)$$

$$H_{(M=1/2\rightarrow M=-1/2)} = (1+1.8up/g)^{-1}[H_o-A(1-1.8Up/A)m] \qquad (A\text{-}6)$$

$$H_{(M=-1/2\rightarrow M=-3/2)} = (1+1.2up/g)^{-1}[H_o-A(1+1.2Up/A) + \frac{A^2}{H_o}m] \qquad (A\text{-}7)$$

where A stands for $(A'/g\beta)$, and A' is the usual hyperfine coupling coefficient.

2. DERIVATION OF u_1 AND U_1

The octahedral crystalline field of MgO and CaO splits the orbital level of V^{2+} to give a singlet Γ_2, lowest lying, and two triplets Γ_4 and Γ_5 as shown in Fig. A-1.

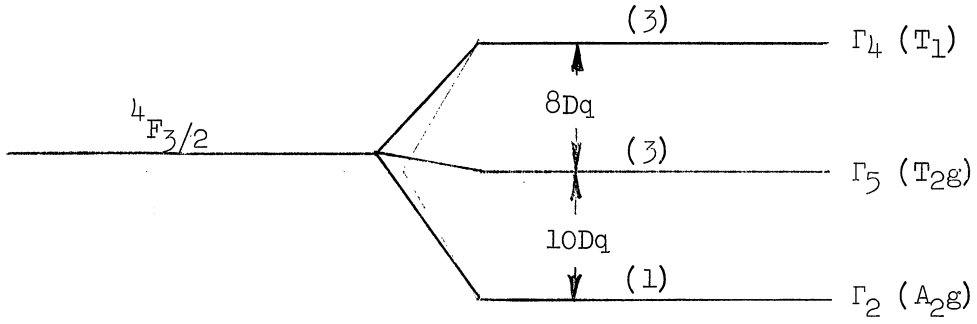

Fig. A-1. Orbital levels of V^{2+} in MgO.

Assuming weak bonding, eigenfunctions of Γ_2, Γ_4, and Γ_5 energy levels are as following

$$|\Gamma_2> = (2)^{-1/2}[\,|2> - |-2>]$$

$$|\Gamma_{41}> = |0>$$
$$|\Gamma_{42}> = (8)^{-1/2}[\sqrt{5}|-3> + \sqrt{3}\,|+1>]$$
$$|\Gamma_{43}> = (8)^{-1/2}[\sqrt{5}\,|3> + \sqrt{3}\,|-1>]$$

$$|\Gamma_{51}> = (2)^{-1/2}[|2> + |-2>]$$
$$|\Gamma_{52}> = (8)^{-1/2}[-\sqrt{3}\,|-3> + \sqrt{5}\,|1>]$$
$$|\Gamma_{53}> = (8)^{-1/2}[-\sqrt{3}\,|3> + \sqrt{5}\,|-1>]$$

The matrix elements of L_+, L_-, and L_z for L=3 with respect to these states are given in Table A-1.

TABLE A-1

MATRIX ELEMENTS OF L_+, L_-, AND L_z FOR L = 3
WITH RESPECT TO Γ_2, Γ_4, AND Γ_5 ENERGY LEVELS

	$\lvert\Gamma_2>$			$\lvert\Gamma_{51}>$			$\lvert\Gamma_{52}>$			$\lvert\Gamma_{53}>$			$\lvert\Gamma_{41}>$			$\lvert\Gamma_{42}>$			$\lvert\Gamma_{43}>$		
	L_z	L_+	L_-	L_z	L_+	L_-	L_z	L_+	L_-	L_z	L_+	L_-	L_z	L_+	L_-	L_z	L_+	L_-	L_z	L_+	L_-
$<\Gamma_2\rvert$	0	0	0	2	0	0	0	$2\sqrt{2}$	0	0	0	$-2\sqrt{2}$	0	0	0	0	0	0	0	0	0
$<\Gamma_{51}\rvert$	2	0	0	0	0	0	0	$\sqrt{2}/2$	0	0	0	$\sqrt{2}/2$	0	0	0	0	$\sqrt{30}/2$	0	0	0	$\sqrt{30}/2$
$<\Gamma_{52}\rvert$	0	0	$2\sqrt{2}$	0	0	$\sqrt{2}/2$	-1/2	0	0	0	0	0	0	$\sqrt{30}/2$	0	$\sqrt{15}/2$	0	0	0	0	0
$<\Gamma_{53}\rvert$	0	$-2\sqrt{2}$	0	0	$\sqrt{2}/2$	0	0	0	0	1/2	0	0	0	0	$\sqrt{30}/2$	0	0	0	$-\sqrt{15}/2$	0	0
$<\Gamma_{41}\rvert$	0	0	0	0	0	0	0	0	$\sqrt{30}/2$	0	$\sqrt{30}/2$	0	0	0	0	0	0	$3\sqrt{2}/2$	0	$3\sqrt{2}/2$	0
$<\Gamma_{42}\rvert$	0	0	0	0	0	$\sqrt{30}/2$	$\sqrt{15}/2$	0	0	0	0	0	0	$3\sqrt{2}/2$	0	-3/2	0	0	0	0	0
$<\Gamma_{43}\rvert$	0	0	0	0	$\sqrt{30}/2$	0	0	0	0	$-\sqrt{15}/2$	0	0	0	0	$3\sqrt{2}/2$	0	0	0	3/2	0	0

For instance, according to this Table $<\Gamma_{53}|L_+|\Gamma_2> = -2\sqrt{2}$. Figure A-2 shows all possible coupling channels among Γ_2, Γ_4, and Γ_5 levels.

Several possible mechanisms contribute to the coefficients u and U in Eq. (A-2). It can be seen that one of the major contributions to u, which lends itself to theoretical calculations, is made by the Zeeman term, $\beta\underline{L}\cdot\underline{H}+2\beta\underline{S}\cdot\underline{H}$ and the spin-orbit coupling term $\lambda\underline{L}\cdot\underline{S}$. We denote this contribution by u_1. Similarly, a major contribution to U comes from the Zeeman term and the hyperfine interaction term $P\underline{L}\cdot\underline{I}$ and is denoted by U_1. Using 4th order perturbation theory, the interaction between these terms and the energy levels of V^{2+} can be calculated.

a. Calculation of u_1

The factor u_1 can be obtained by computing the numerical coefficient

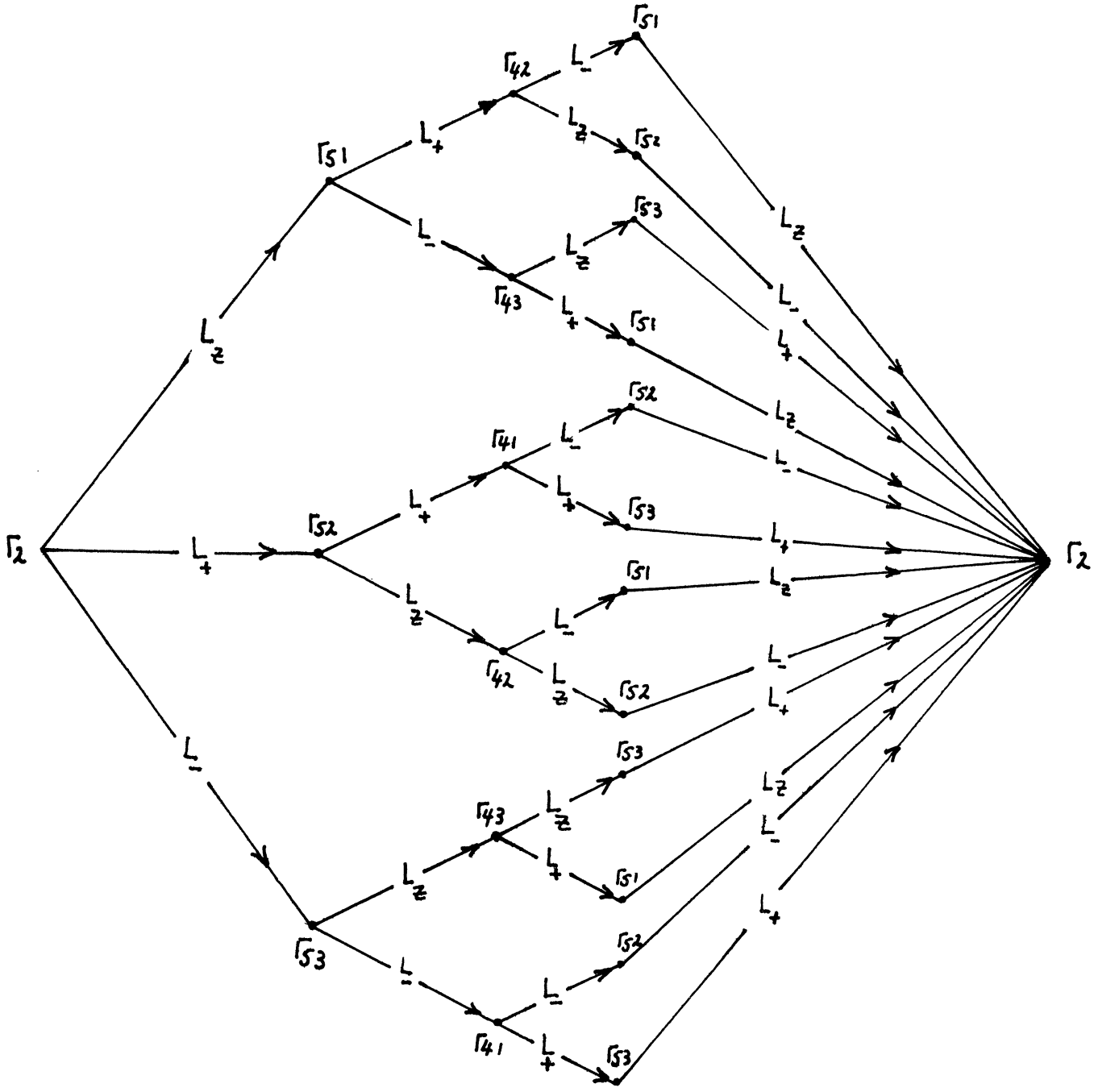

Fig. A-2. Coupling channels.

of either $\beta S_x^3 H_x^3$, $\beta S_y^3 H_y$, or $\beta S_z^3 H_z^3$ in Eq. (A-2). In order to do this, we use the 4th order perturbation calculations to determine the interactions between the perturbation Hamiltonian

$$V_1 = \beta(\underline{L}+2\underline{S})\cdot\underline{H} + \lambda\underline{L}\cdot\underline{S} \qquad (A\text{-}8)$$

and the orbital triplets.* The coefficient u_1 can be found by collecting terms of first order in H and 3rd order in S. The term $2\beta\underline{S}\cdot\underline{H}$ in Eq. (A-8) does not contribute anything to u_1 and hence it can be excluded from V_1. The simplified perturbation Hamiltonian can be then written as,

$$v_1 = \beta\underline{L}\cdot\underline{H} + \lambda\underline{L}\cdot\underline{S} \qquad (A\text{-}9)$$

The 4th order perturbation formula for non-degenerate ground state is

$$W_4 = -\sum_{k,m,q}\sum_{j,\ell,p}{}' \frac{\langle \Gamma_r|V|\Gamma_{j,k}\rangle\langle \Gamma_{j,k}|V|\Gamma_{\ell,m}\rangle\langle \Gamma_{\ell,m}|V|\Gamma_{pq}\rangle\langle \Gamma_{pq}|V|\Gamma_r\rangle}{(E_j-E_r)(E_\ell-E_r)(E_p-E_r)}$$

$$+\sum_{\ell,m}{}' \frac{|\langle \Gamma_r|V|\Gamma_{\ell,m}\rangle|^2}{E_\ell-E_r}\sum_{j,k}{}' \frac{|\langle \Gamma_{j,k}|V|\Gamma_r\rangle|^2}{(E_j-E_r)^2}$$

$$+\langle \Gamma_r|V|\Gamma_r\rangle \sum_{j,k}{}'\sum_{\ell,m}{}' \left(\frac{1}{E_\ell-E_r}+\frac{1}{E_j-E_r}\right)\left(\frac{\langle\Gamma_r|V|\Gamma_{j,k}\rangle\langle\Gamma_{j,k}|V|\Gamma_{\ell,m}\rangle\langle\Gamma_{\ell,m}|V|\Gamma_r\rangle}{(E_j-E_r)(E_\ell-E_r)}\right)$$

$$-|\langle \Gamma_r|V|\Gamma_r\rangle|^2 \sum_{j,k}{}' \frac{\langle \Gamma_r|V|\Gamma_{j,k}\rangle\langle \Gamma_{j,k}|V|\Gamma_r\rangle}{(E_j-E_r)^3} \qquad (A\text{-}10)$$

*It may seem that another source of contribution to u_1 arises from $2\beta\underline{S}\cdot\underline{H}$ in first order along with $\lambda\underline{L}\cdot\underline{S}$ in second order. However, the result of third order calculation for these perturbation operators is zero.

where $|\Gamma_r>$ and E_r denote the ground level wave function and energy respectively and the prime on Σ denotes the omission of the terms with index r from the summation.

The last two terms of Eq. (A-10) have vanishing result in our case because

$$<\Gamma_r|v_1|\Gamma_r> = 0$$

Hence, the 4th order perturbation formula, Eq. (A-10), reduces to

$$W_4 = W_4' + W_4'' \qquad \text{(A-11)}$$

where

$$W_4' = -\sum_{k,m,q}\sum_{j,\ell,p}{}' \frac{<\Gamma_r|V|\Gamma_{j,k}><\Gamma_{j,k}|V|\Gamma_{\ell,m}><\Gamma_{\ell,m}|V|\Gamma_{pq}><\Gamma_{pq}|V|\Gamma_r>}{(E_j-E_r)(E_\ell-E_r)(E_p-E_r)} \qquad \text{(A-12)}$$

and,

$$W_4'' = \sum_{\ell,m}{}' \frac{|<\Gamma_r|V|\Gamma_{\ell,m}>|^2}{E_\ell-E_r} \sum_{j,k}{}' \frac{|<\Gamma_{j,k}|V|\Gamma_r>|^2}{(E_j-E_r)^2} \qquad \text{(A-13)}$$

Furthermore, we can show that components $S_x^3 H_x$, etc., can not be obtained from W_4'' and therefore this part of the perturbation formula is not needed for calculation of u_1. To prove this, first we notice that W_4'' can mix Γ_2 and Γ_5 levels only because matrix elements of v_1 with respect to Γ_2 and all Γ_4 levels are zero. Now, using shift operators

$$L_{\pm} = L_x \pm iL_y$$

$$S_{\pm} = S_x \pm iS_y$$

the perturbation operator v_1 can be written as

$$v_1 = \beta[L_zH_z + \frac{1}{2}(L_+H_-+L_-H_+)] + \lambda[L_zS_z + \frac{1}{2}(L_+S_-+L_-S_+)] \qquad (A\text{-}14)$$

Using (A-14) in W_4'' we obtain

$$W_4'' = [|(\beta H_z+\lambda S_z) < \Gamma_2|L_z|\Gamma_{51} >|^2$$

$$+ \frac{1}{4}|\beta H_-+\lambda S_-|^2 < \Gamma_2|L_+|\Gamma_{52} >< \Gamma_{52}|L_-|\Gamma_2 >$$

$$+ \frac{1}{4}|\beta H_+ + \lambda S_+|^2 < \Gamma_2|L|\Gamma_{53} >< \Gamma_{53}|L_+|\Gamma_2 >]^2 \qquad (A\text{-}15)$$

Replacing the matrix elements in (A-15) by their values from Table A-1 we have

$$W_4'' = 4[2(\beta H_z+\lambda S_z)^2 + |\beta H_-+\lambda S_-|^2 + |\beta H_+ + \lambda S_+|^2]^2 \qquad (A\text{-}16)$$

Expanding (A-16) and making use of relationships

$$S_zH_z + \frac{1}{2}(S_-H_+ + S_+H_-) = \underline{S}\cdot\underline{H}$$

and

$$S_-S_+ + S_+S_- = 2S(S+1) - 2S_z^2$$

we find,

$$W_4'' = \frac{64\beta\lambda^3}{E_{52}^3}[\underline{S}\cdot\underline{H}(S+1)S] + w \qquad (A\text{-}17)$$

where w denotes the terms of second 4th power in s and in H, and E_{52} stands for E_5-E_2.

We notice that W_4'' does not contain explicitly terms such as $S_x^3H_x$, $S_y^3H_y$, etc. It has rather the form of the 4th term in Eq. (A-2). Therefore, to calculate u_1 we must apply W_4' to the perturbation Hamiltonian v_1. But first we consider that

$$S_x^3H_x = \frac{1}{16}(S_+ + S_-)^3(H_+ + H_-)$$

$$S_y^3H_y = \frac{1}{16}(S_+ - S_-)^3(H_+ - H_-)$$

Hence,

$$S_x^3H_x+S_y^3H_y+S_z^3H_z = \frac{1}{8}[(S_+^3+S_+S_-^2+S_-S_+S_-+S_-^2S_+)H_+ + (S_-^3+S_+^2S_-+S_+S_-S_++S_-S_+^2)H_-] + S_z^3H_z \qquad (A\text{-}18)$$

Replacing S_- in the first parenthesis by S_+-2iS_y, and S_+ in the second parenthesis by S_-+2iS_y (A-18) can be written as,

$$S_x^3H_x+S_y^3H_y+S_z^3H_z = \frac{1}{2}(S_+^3H_+ + S_-^3H_-) + S_z^3H_z + R \qquad (A\text{-}19)$$

where R represents the terms not reducible to either $S_+^3H_+$, $S_-^3H_-$, or $S_z^3H_z$.

Comparing (A-19) with (A-2) it is easily seen that u_1 can be found by applying the 4th order perturbation calculations (W_4' part) to v_1 and determining the coefficient of any term of the right side of Eq. (A-19). However, the first two terms are much easier than the others to deal with and thus we will do the calculations for $S_x^3H_x$. The perturbation Hamiltonian reveals

that this term can only come from operators such as $(\lambda L_- S_+)^{(3)}(\beta L_- H_+)$. According to Fig. 2-A the only chain through which operator $L_-^{(4)}$ can interact with the energy levels is

$$< \Gamma_2|L_-|\Gamma_{53} >< \Gamma_{53}|L_-|\Gamma_{41} >< \Gamma_{41}|L_-|\Gamma_{52} >< \Gamma_{52}|L_-|\Gamma_2 > \qquad \text{(A-20)}$$

However, since L_-H_+ can occupy any of the four channels in the chain (A-20), there are effectively four chains similar to (A-20). Using the scheme (A-20) in W_4' and taking the factor of 4 into account we obtain

$$-\frac{4\beta\lambda^3}{E_{52}^2 E_{42}} S_+^3 H_+ < \Gamma_2|L_-|\Gamma_{53} >< \Gamma_{53}|L_-|\Gamma_{41} >< \Gamma_{41}|L_-|\Gamma_{52} >< \Gamma_{52}|L_-|\Gamma_2 > \qquad \text{(A-21)}$$

Table A-1 gives the values of the matrix elements

$$< \Gamma_2|L_-|\Gamma_{53} > = -2\sqrt{2}$$
$$< \Gamma_{53}|L_-|\Gamma_{41} > = \sqrt{30}/2$$
$$< \Gamma_{41}|L_-|\Gamma_{52} > = \sqrt{30}/2$$
$$< \Gamma_{52}|L_-|\Gamma_2 > = 2\sqrt{2}$$

Hence, the coefficient of $\beta S_+^3 H_+$ is obtained from (A-21) to be $240\lambda^3/E_{52}^2 E_{42}$ and so,

$$u_1 = \frac{1}{2} \times \frac{240\lambda^3}{E_{52}^2 E_{42}}$$

or,

$$u_1 = \frac{120\lambda^3}{E_{52}^2 E_{42}} \qquad \text{(A-22)}$$

b. Calculation of U_1

If in the perturbation calculations $\beta \underline{L} \cdot \underline{H}$ is replaced by $P\underline{L} \cdot \underline{I}$ we obtain the coefficient U_1. However, since as far as operation on the orbital levels is concerned $\underline{I}$ can be regarded as a constant similar to $\underline{H}$ the two coefficients u_1 and U_1 are equal within a constant factor P. That is,

$$U_1 = Pu_1 \qquad \text{(A-23)}$$

APPENDIX B

THE SHIFT IN THE g-FACTOR

Since in an octahedral field g is isotropic,

$$g_x = g_y = g_z$$

The Zeeman term and spin-orbit coupling term may be written as (with $\underline{H} \| z\text{-axis}$)

$$H = \beta(L_z H_z + 2S_z H_z) + \lambda \underline{L} \cdot \underline{S}$$

As we have seen before since all matrix elements of $\underline{L}$ with respect to Γ_2 and Γ_4 levels are zero, we have only to deal with Γ_2 and Γ_5 interactions.

To the first order

$$W_1 = \langle \Gamma_2 | H | \Gamma_2 \rangle = 2\beta S_z H_z$$

To the second order approximation we have two possible chains,

Thus,

$$W_2 = -2 \frac{\beta\lambda}{E_{52}} \langle \Gamma_2 | L_z H_z | \Gamma_{51} \rangle \langle \Gamma_{51} | L_z S_z | \Gamma_2 \rangle$$

$$W_2 = -\frac{8\lambda\beta}{E_{52}} S_z H_z$$

Neglecting the higher order approximations we have

$$W_1 + W_2 = 2\beta S_z H_z - \frac{8\beta\lambda}{E_{52}} S_z H_z = \left(2\beta - \frac{8\lambda\beta}{E_{52}}\right) S_z H_z$$

Comparing this expression with the Zeeman term in spin Hamiltonian

$$H_S = g\beta S_z H_z + \ldots$$

we find

$$g\beta = \left(2\beta - \frac{8\lambda\beta}{E_{52}}\right)$$

or

$$g-2 = -\frac{8\lambda}{E_{52}} \qquad \text{(B-1)}$$

Now from Eq. (A-22),

$$\lambda^3 = \frac{u_1 E_{52}^2 E_{42}}{120} \qquad \text{(B-2)}$$

Eliminating λ between (B-1) and (B-2) and use $E_{52}/E_{42} = 5/9$ we get,

$$u_1 = -\frac{25}{192}(g-2)^3 \qquad \text{(B-3)}$$

REFERENCES

1. J. E. Wertz, J. L. Vivo and B. Musulin, Phys. Rev. 100, 1810A (1955).

2. W. Low, Phys. Rev. 101, 1827 (1956).

3. J. E. Wertz, P. Auzins, J.H.E. Griffith and J. W. Orton, Farad Soc. Disc. 26, 66 (1958).

4. W. Low, The New York Acad. of Sci. 72, 69 (1958).

5. J. E. Wertz, J. W. Orton and P. Auzins, J. Appl. Phys. 33, Suppl. 1, 322 (1962).

6. G. H. Azarbayejani and C. Kikuchi, Bull. Am. Phys. Soc., Seri II, 8, 344 (1963).

7. A. J. Shuskus, Phys. Rev. 127, 1529 (1962).

8. F. S. Ham, G. W. Ludwig, G. D. Watkins and H. H. Woodbury, Phys. Rev. Letters 5, 468 (1960).

9. J. Lambe and R. Ager, Rev. Sci. Inst. 30, 599 (1959).

10. H. H. Woodbury and G. W. Ludwig, Phys. Rev. 117, 102 (1960).

11. M. D. Sturge, Phys. Rev. 130, 639 (1963).

12. C. E. Moore, Atomic Energy Levels, Nat. Bur. Stands., Circ. 467.

13. Mattarese and C. Kikuchi, J. Phys. and Chem. Solids. 1, 117 (1956).

14. M. Dvir and W. Low, Proc. Phys. Soc. (London) 75, 136 (1960).

15. B. Bleaney, Proc. Phys. Soc. (London) A73, 939 (1959).

16. F. Koster and H. Statz, Phys. Rev. 113, 445 (1959).